Journal of Organometallic Chemistry 791 (2015) 183–191

Contents lists available at ScienceDirect

Journal of Organometallic Chemistry

journal homepage: www.elsevier.com/locate/jorganchem

Silver(I), Gold(I) and Gold(III)-N-Heterocyclic carbene complexes of naphthyl substituted annelated ligand: Synthesis, structure and cytotoxicity

Tapastaru Samanta [a, 1], Rudra Narayan Munda [b, 1], Gourisankar Roymahapatra [c], Abhishek Nandy [d], Krishna Das Saha [d, *], Salem S. Al-Deyab [e], Joydev Dinda [f, *]

[a] School of Applied Science, Haldia Institute of Technology, Haldia, 721657, Purba Medinipur, West Bengal, India
[b] Department of Biotechnology, North Orissa University, Takatpur, Baripada, Mayurbhanj, 757003, Odisha, India
[c] Department of Basic Science, Global Institute of Science and Technology, ICARE Complex, Haldia, 721 657, Purba Medinipur, West Bengal, India
[d] Cancer Biology and Inflammatory Disorder Division, CSIR-Indian Institute of Chemical Biology, Jadavpur, Kolkata, 700032, West Bengal, India
[e] Chemistry Department, College of Science, King Saud University, B.O. Box 2455, Riyadh, 11451, Saudi Arabia
[f] Department of Chemistry, ITM University, Gwalior, MP, India

ARTICLE INFO

Article history:
Received 3 March 2015
Received in revised form
3 May 2015
Accepted 11 May 2015
Available online 28 May 2015

Keywords:
N-heterocyclic carbene
Annelated carbene
Disproportion
Silver-NHC
Gold-NHC

ABSTRACT

The new type of annulated imidazolium salt 1-naphthyl-2-pyridin-2-yl-2*H*-imidazo[1,5-*a*]pyridin-4-ylium hexafluorophosphate (**1**·HPF_6) and three novel N-heterocyclic carbene complexes (NHCs) [Ag(**1**)$_2$][PF_6] (**2**), [Au(**1**)$_2$][PF_6] (**3**), and [Au(**1**)Cl_3] **4** have been synthesized and characterized by different spectroscopic techniques. The solid state structure of **2** has been determined by single crystal X-ray diffraction studies. The complex **3** has been synthesized *via* trans-metallation, whereas complex **4** was obtained *via* a disproportionation process. The cytotoxicities of the complexes **2**, **3** and **4** were tested *in vitro* against non-small lung carcinoma (A549), colorectal carcinoma (HCT-116) and breast adenocarcinoma (MCF-7) cell lines. The measured IC_{50} values showed that the Au (I) complex **3** is more potent than the complexes **2** and **4** as well as cisplatin.

1. Introduction

Ever since the successful isolation of a stable crystalline N-heterocyclic carbene (NHC) in 1991 by Arduengo, it has remained as a powerful class of carbon-based ligands [1] studied for 'chemical curiosity'. N-heterocyclic carbenes are an established class of ligands for a broad range of transition metals and are relatively easy to synthesize, tune and modify [2]. Due to their strong σ-donor and weak π-accepting properties, NHCs often form stable organometallic complexes with a broad spectrum of transition and non-transition metals in different oxidation states [3]. Currently, research in this field is focussed on three main directions: (i) the development of novel NHC ligands [4], (ii) applications of metal-NHCs in catalysis and materials science [5] and (iii) the use of NHC complexes as drugs for biomedical applications [6].

The metal based drugs, where metal plays an important role, occupy a prominent place in pharmaceutical chemistry; this has been highlighted in many reviews [7]. Recent studies of NHC complexes as anticancer agents have opened the door to another emerging field, search for alternatives to cisplatin or $PtCl_2(NH_3)_2$ [8] which has been used for a long time but needs to be substituted because of several drawbacks along with nephrotoxicity [7]. Recent findings have established that Ag–NHCs possess useful antibacterial and anticancer properties [9]. However, the big problem with the existing silver drugs is that they lose their effects quickly due to rapid release of the Ag^+ ions. This problem can be solved by introducing gold in place of silver [10]. The application of gold in medicine was started several thousand years ago in China and gold complexes have been evaluated for many different pharmaceutical purposes, notably cancer and arthritis [10]. The spectrum of gold complexes with described cell growth inhibiting properties comprises a large variety of different ligands attached to gold in the oxidation states + I or + III [11]. The gold (I) phosphine complex

* Corresponding authors.
E-mail addresses: dindajoy@yahoo.com, joydevdinda@gmail.com (J. Dinda).
[1] Both Tapastaru Samanta and Rudra Narayan Munda have contributed equally to this work.

http://dx.doi.org/10.1016/j.jorganchem.2015.05.049
0022-328X/

auranofin, which was initially developed as an anti-rheumatic agent, was shown to have potential as an anticancer agent. Unfortunately, auranofin is readily metabolized by natural thiols, and this significantly restricts its activity [12]. To increase the stability of gold complexes under biologically relevant conditions, attention has been directed toward the synthesis and study of analogous complexes bearing stabilizing NHC ligands [13]. Metal-NHC complexes can be synthesized *via* free carbene, in situ and using transmetallation methods; undoubtedly, the use of silver–carbene complexes as carbene transfer reagent for the synthesis of other metal complexes is one of the most convenient ways to avoid harsh conditions, wherein azolium salts react directly with metal salts [14]. The gold (III)–NHC complex was synthesized by disproportionation method developed by our group [15].

Owing to their electronic tunability, the NHCs have been integrated into a large variety of metal complexes [16]. The electronic properties of NHC complexes can be altered by modifying C (1/5)/C (3/4) or C (4/5) in the ligand side and by N-substitution [16], as well as by changing the nature of the transition metal [17]. Use of donor-functionalization to develop new classes of NHC ligands, including weak donor functionalized NHCs (wdf-NHC), has also played an important role in organometallic chemistry [18]. Interest in the development of new polycyclic aromatic annulated imidazol-2-ylidenes [19] and their corresponding transition metal complexes has arisen due to their potential application in catalysis, fluorescent devices and biological applications. Our group has recently reported pyridine/pyrimidine functionalized annelated NHC complexes [18,19] with various applications. Inspired by these and other recent findings, we decided to develop naphthyl wingtip annelated NHCs.

2. Results and discussion

2.1. Synthetic strategy

Ag(I) metal complexes of the Schiff's base 2-pyridylnaphthylmethyleneamine and their photoluminescence have been described earlier [20]; we have now subjected the Schiff base to formylative cyclization to synthesize the new class of pro-ligand 1-naphthyl-2-pyridin-2-yl-2*H*-imidazo[1,5-*a*]pyridin-4-ylium hexafluorophosphate (**1·HPF$_6$**). The salt **1·HPF$_6$** was synthesized 2-naphthyl-*N*-(2-pyridine)methylamine and paraformaldehyde with 2(N) HCl under standard conditions, followed by anion metathesis with NH_4PF_6 [19]. As expected, the singlet proton signal of imidazolium-C2H atom appeared at low field (10.12 ppm), indicating its relatively high acidity compared to other protons. Formation of **1·HPF$_6$** was also confirmed from appearance of a carbene carbon signal (NCN) at 148.5 ppm similar to other annulated carbenes reported so far by our group [19]. Treatment of Ag_2O with **1·HPF$_6$** afforded the Ag(I)–NHC complex **2** (Scheme 1), as determined by the absence of the diagnostic ^{1}H NMR signal associated with the imidazolium precursor (δ = 10.12 ppm (s); DMSO-d_6). In addition, the spectrum revealed only one singlet at 8.67 ppm also supporting the Ag–C coordination. Although Ag–C coupling was not observed, a singlet was recorded at 170.6 ppm in ^{13}C NMR spectrum of a solution of **2** and attributed to a carbene center. The formation of a complex coordinated to two ligands was supported by mass spectrometry, which revealed a signal consistent with a $[Ag(\mathbf{1})_2]^+$ ion (m/z = 595.8). Additional support for the structure of **2** was obtained *via* single crystal X-ray crystallography. As shown in Fig. 1, the solid state structure of **2** revealed that two carbene centers were coordinated to the Ag center and Ag(I)–C distance varies in the region 2.070(3)–2.072(4) Å, shorter than reported for the annelated biscarbene silver complex of 2-pyridin-2-yl-2*H*-imidazo[1,5-*a*]pyridin-4-ylium hexafluorophosphate by our group [2.086(7) Å] [21]. Additional crystallographic details are summarized in Table 1 and discussed below.

The complex Au(SMe$_2$)Cl was successfully transmetalated with **2** to afford Au(I)–NHC (**3**). In agreement with the structure shown in Scheme 1, complex **3** displayed a ^{13}C NMR signal at 174.6 ppm and a mass spectrometric signal at m/z 685.2, consistent with a $[Au(\mathbf{1})_2]^+$ ion. We synthesized the Au(III)–NHC complex (**4**) as shown in Scheme 1 using **3** and Au(SMe$_2$)Cl, capitalizing on disproportionation reaction, a protocol that has been first reported by our group [15]. Upon stirring a colorless acetonitrile solution of the Au(I)–NHC complex (**3**) and Au(SMe$_2$)Cl at room temperature for 5–6 h, an orange/yellow color formed along with the appearance of a yellow precipitate of Au (0); the latter may be reconverted to Au(SMe$_2$)Cl.

After separation and purification, the yellow product was analyzed by NMR spectroscopy. Although the ^{1}H NMR spectrum of the isolated solid was similar to that recorded for complex **3**, the former displayed a relatively upfield ^{13}C NMR signal at δ = 159.7 ppm, which was subsequently assigned to a $C_{carbene}$ atom coordinated to a Au(III) center. For comparison, the ^{13}C NMR resonance observed for the $C_{carbene}$ atom in the isolated material was slightly downfield with respect to the NCHN signal recorded for the parent imidazolium salt (148.5 ppm), but consistent with analogous signals displayed by [AuX$_3$(NHC)] complexes bearing imidazolin-2-ylidene or imidazolidin-2-ylidene ligands [11,21]. The isolated material was also studied by mass spectrometry, which revealed signals consistent with $[Au(\mathbf{1})Cl_2]^+$ (m/z of 463) and $[Au(\mathbf{1})Cl]^{2+}$ (m/z of 427.5). Collectively, these results support the structure shown in Scheme 1.

2.2. X-ray crystal structure of **2**

Complex **2** was obtained in crystalline form by slow diffusion of diethyl ether into an acetonitrile solution of the complex. Molecular structure of **1** is shown in Fig. 1. The crystallographic data and the selected metrical data are listed in Table 1. In the complex, the silver center has linear geometry, being covalently bound to two NHC ligands. The Ag-$C_{carbene}$ bond distances, Ag(1)–C(1) = 2.072(3) and Ag(1) – C(18) = 2.070(4) Å, are shorter than but close to the average value 2.05 Å [9] reported so far for similar complexes, and shorter than the Ag–C_{carb} sum of the covalent radii 2.111 Å. The experimental bond parameters are compared with the theoretical data listed in Table 2. The theoretical bond parameters are very consistence with the experimental data. The molecule possesses π–π stacking interaction (3.833 Å) through aromatic rings (shown in Fig. 2). The angle at silver [C(1)–Ag(1)–C (18)] is almost linear [175.77(14)]; the N1–C1–N2 and N3–C18–N4 [(N–C_{carb}–N)] angles, 104.5(3) and 103.4(3)° respectively, are shorter than that observed in the bis carbene system developed by our group [21]. Renso et al. [22] had observed that the (N–C_{carb}–N) angle is larger in case of (saturated NHC)–silver complexes in comparison to the unsaturated NHC–silver complexes. This is attributed to the different ring geometries of the 4,5-dihydroimidazole ring in the saturated NHC complex as opposed to that of the imidazole ring in the NHC complex. The dihedral angle between the naphthyl ring and the annulated imidazole ring varies from 66.38° to 67.09°, whereas that between two annulated groups and two naphthyl rings are 34.58° and 28.15° respectively.

2.3. Theoretical studies and electronic properties

We applied density functional theory (DFT) to complexes **2, 3** and **4** to understand the nature of the orbitals and to explain the electronic properties. Geometries of the synthesized complexes were optimized for the structure. Full molecular geometry

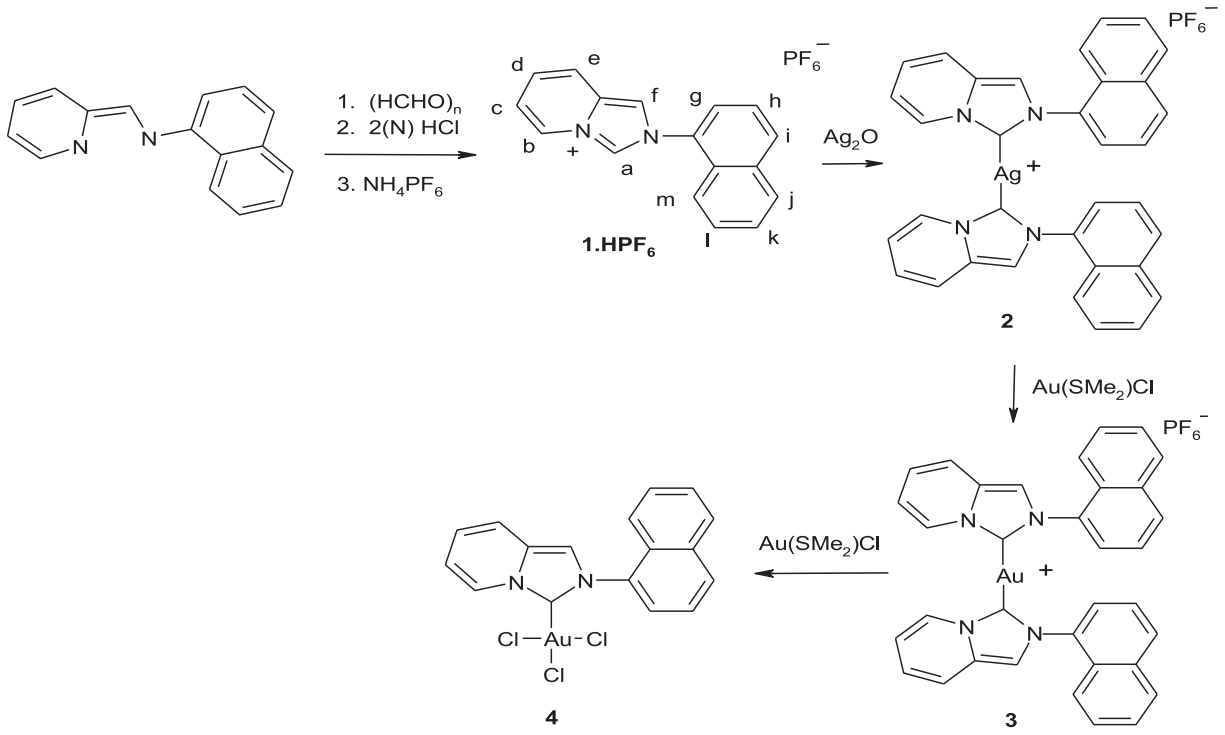

Scheme 1. Synthesis of various NHC complexes. The letters surrounding the structure of **1** refer to the NMR assignments; see the Experimental Section.

optimizations were carried out at the Becke3LYP (B3LYP) level [23] using LANL2DZ basis set of DFT. The number of imaginary frequencies of **2, 3** and **4** was zero, implying that the structures correspond to minimum energy ones on the potential energy surface. Frontier molecular orbitals were generated using GV03 at the same level of theory (as shown in Fig. 3). The theoretical Au(I)–C_{carb} bond lengths varies 2.070–2.070 Å, where as Au(III)–C_{carb} distance is 2.026 Å (Table 2), consistance with the gold-C_{carb}

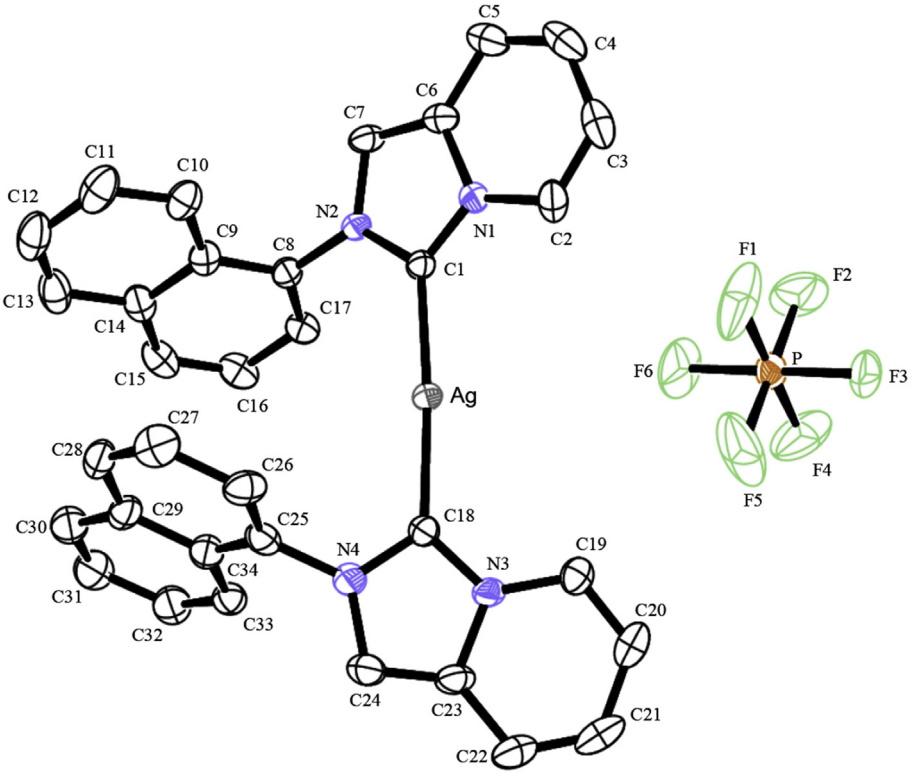

Fig. 1. ORTEP diagram of **2** shown at the 30% probability level. The H atoms have been removed for clarity.

Table 1
Summary of Crystallographic data of **2**.

	Complex 2
Empirical formula	$C_{34}H_{24}AgF_6N_4P$
Formula weight	741.41
Crystal system	Triclinic
Space group	P-1
Temperature (K)	120(2)
Cell dimensions	
a (Å)	8.3814(2)
b (Å)	11.7084(2)
c (Å)	15.3158(3
α(°)	96.7059(11)
β(°)	92.7517(11)
γ(°)	97.1961(12)
Volume (Å^3)	1477.945(52)
Z	2
Density (Mg m^{-3})	1.666
Absorption coefficient (μ)	0.807
F(000)	744
Crystal size (mm)	0.2 × 0.19 × 0.18
Theta range for data collection	3.02–27.50
Index ranges	$-10 \le h \le 10$;$-15 \le k \le 15$;$-19 \le l \le 19$
Reflections collected	32091
Independent reflections	6778[*R*(int) 0.0214]
No. of parameters refined	415
R indices (all data)	R1 = 0.0547, wR2 = 0.1268
Final *R* indices [$I > 2\sigma(I)$]	R1 = 0.0518, wR2 = 0.1221
Largest diff. peak and hole (e Å^{-3})	3.40 and −2.25
GOF	1.118

annelated system reported by our group [11].

The UV–Vis spectra of the proligand in acetonitrile showed peaks at 234, 245 and 320 nm; the lower wave length frequencies were assigned to intra and inter ligand charge transfer and the higher one was attributed to MLCT. Estimation of frontier orbital contribution and the data in Fig. 3 also support the MLCT. Close inspection of FMO revealed that the electronic population of HOMO lies mainly on the annulated carbene part, whereas in case of LUMO it is in the naphthyl ring part as shown in Fig. 3. The UV–Vis absorption spectrum of **2** is similar to that of **1**, with peaks appearing at 232, 247 and 347 nm in the same solvent; tha major difference in case of **2** is that the higher wavelength λ_{max} appears red (in the web version) shifted to 347 nm, ostensibly due to MLCT. Complexes **3** and **4** show the corresponding λ_{max} at 352 and 350 nm respectively. All the complexes show weak luminescence at $\lambda_{max}^{emission}$ *ca*

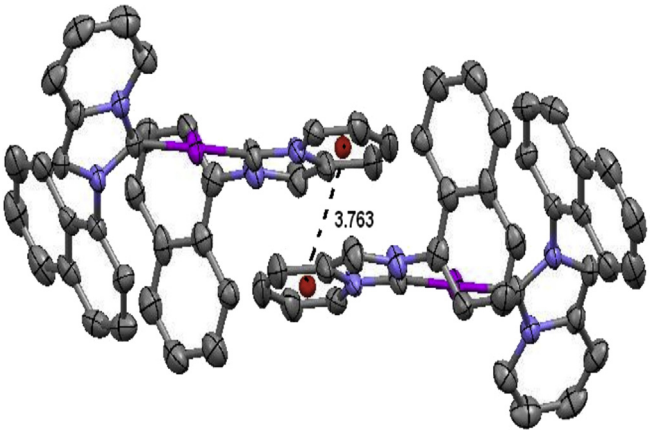

Fig. 2. π–π stacking interactions of arene rings of **2.**

430–520 nm. The proligand is also weakly luminescent, but the intensity increases with complexation and maximum $\lambda_{max}^{emission}$ was observed in case of Au–NHC, **3**. The intense emission band centered at 430 nm corresponds to intraligand transitions.

2.4. Biological evaluation

2.4.1. Growth inhibitory effect of complexes 2, 3 and 4

Growth inhibitory effect of complexes **2**, **3** and **4** was observed (shown in Fig. 4) on three cancer cell lines of human origin, namely, non small lung carcinoma cell line (A549), colorectal carcinoma cell line (HCT-116) and breast adenocarcinoma cell line (MCF-7) for 24 h as described earlier and compared to that of cisplatin [11]. Complex **3** was found to be more potent than complexes **2** and **4** towards all the cell lines, with highest growth inhibitory potential towards A549. Both complexes **3** and **4** showed higher growth inhibitory potential towards cancer cell lines as compared to cisplatin. As summarized in Table 3, the IC_{50} values measured for **3** were found to be nearly three times lower than for cisplatin, and generally lower than that of the gold(III) complex **4**. Collectively, these results show less potency of the complexes than those of Au(I)/Au(III)–NHC complexes previous reported by our group [11,21,24]. However, the proligand **1** showed negligible cytotoxicity towards the cancer cells, and the complexes themselves showed (Table 3)

Table 2
Experimental and theoretical bond lengths (Å) and bond angles (°).

Com-plex	Experimental		Theoretical	
	Bond lengths	Bond angles	Bond lengths	Bond angles
2	C(1)–Ag(1) = 2.072(4) C(18)–Ag(1) = 2.070(3) C(1)–N(1) = 1.367(5) C(1)–N(2) = 1.367(5) C(18)–N(3) = 1.357(5) C(18)–N(4) = 1.359(4)	C(1)–Ag(1)–C(18) = 175.8(4) N(1)–C(1)–N(2) = 104.5(3) N(3)–C(18)–N(4) = 103.4(3)	C(2)–Ag(1) = 2.072 C(3)–Ag(1) = 2.070 C(2)–N(11) = 1.367 C(2)–N(14) = 1.368 C(3)–N(4) = 1.356 C(3)–N(10) = 1.357	C(2)–Ag(1)–C(13) = 175.76 N(11)–C(2)–N(14) = 104.4 N(4)–C(3)–N(10) = 103.4
3	–	–	C(1)–Au(70) = 2.072 C(1)–N(13) = 1.368 C(1)–N(10) = 1.367 C(2)–N(3) = 1.360 C(2)–N(9) = 1.357 C(2)–Au(70) = 2.070	C(1)–Au(70)–C(2) = 175.76 N(10)–C(1)–N(13) = 104.43 N(3)–C(2)–N(9) = 104.43
4	–	–	C(10)–N(12) = 1.372 C(10)–N(13) = 1.365 C(10)–Au(32) = 2.026 Au(32)–Cl(33) = 2.439 Au(32)–Cl(34) = 2.418 Au(32)–Cl(35) = 2.429	N(10)–C(1)–N(13) = 104.43 C(10)–Au(32)–Cl(34) = 179.92 Cl(33)-Au(32)-Cl(35) = 173.98 Cl(33)–Au(32)–Cl(34) = 92.72 Cl(35)–Au(32)–Cl(34) = 92.84 C(10)–Au(32)–Cl(33) = 87.27 C(10)–Au(32)–Cl(35) = 87.12

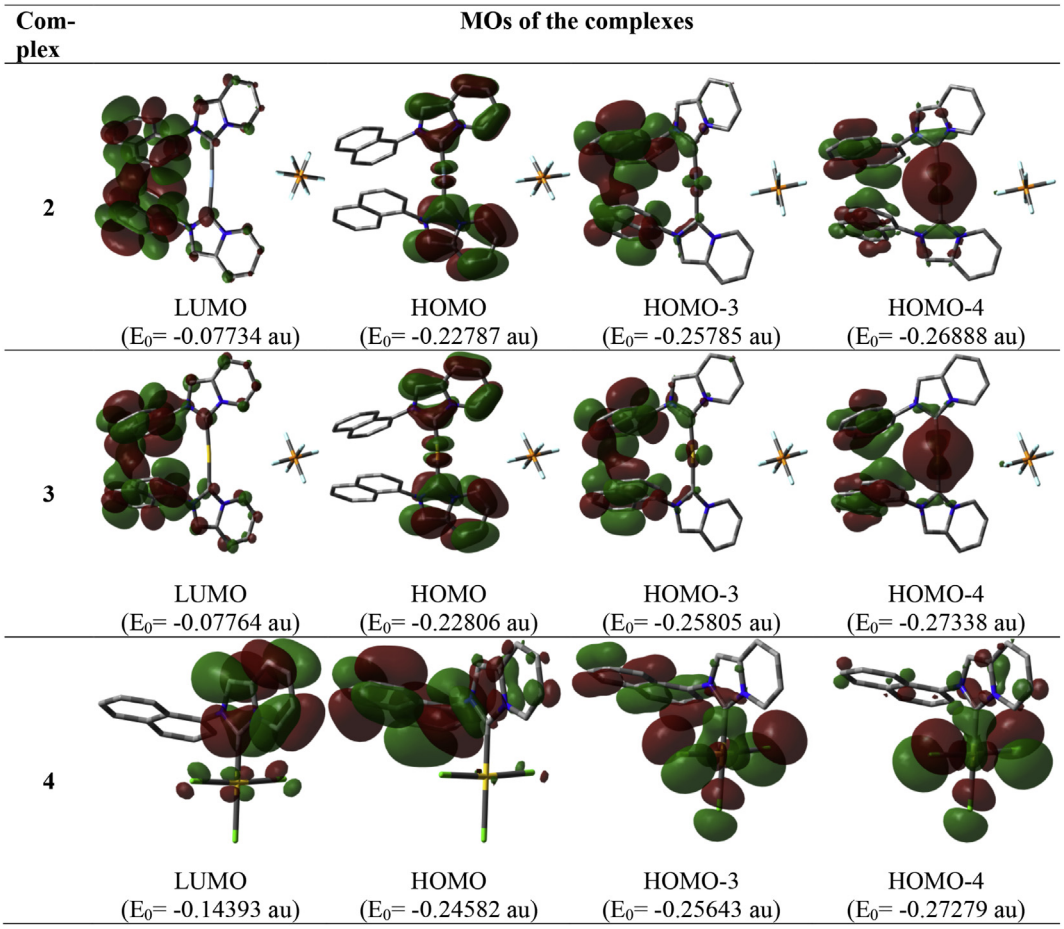

Fig. 3. Some important frontier molecular orbitals of **2, 3** and **4** generated at Gauss View.

negligible cytotoxicity towards human peripheral blood mononuclear cells (PBMCs).

Over the past couple of decades, a broad range of silver(I) complexes supported by NHCs has been synthesized [25] and applied for biological screening [26]. More recently, Ag(I)–NHC complexes were found to be potent agents against drug-resistant pathogens [27,28] and recent studies by Youngs and others have shown that Ag–NHCs are useful in antibacterial and anticancer applications [28]. The common way of modes of action particularly *via* the release of Ag^{+} ions that enters into the cell membranes and disrupts their functions. However, quick release of Ag from Ag-based drugs loses their effectiveness. This limitation was overcome through the use of NHCs as ancillary ligand which strongly binds to metals. Besides silver, gold is also found potent in biomedical field. Gold has been used for centuries in various Chinese medicines. More recently, gold drugs like auranofin has been investigated for their activities against cancer and arthritis, though it was initially developed as an anti-rheumatic agent [29]. Unfortunately, auranofin is readily metabolized by reaction with natural thiols, which restricts its activity [30]. To increase the stability of gold complexes under biologically relevant conditions, NHC ligands have been introduce in place of phosphines [31]. Berners-Price and Barnard obtained very good results against mouse cancer cells using a Au(I)–NHC complex [32]. Panda and Ghosh also successfully developed a Au(I)–NHC complex that exhibited excellent efficiency against HeLa cell proliferation [33]. Filipovska et al. established a new approach to mitochondria targeted antitumor agents using Au(I)–N-heterocyclic carbene compounds [34]. Mohr, Che and Ott also describe the excellent efficiency of Au–NHC against different cancer cell proliferation [35–37]. It is also observed from structure–activity relationship that, the inhibitory potency of Au(I)–NHC complexes may be increased through the incorporation of chloride ligands as opposed to the use of two NHCs [37,38]. Young's showed that, Ag–NHC complexes derived from 4,5-dichloro-1H-imidazole are potent against ovarian (OVCAR-3) and breast (MB157) cancer cells *in vitro*. Same group prepared bis[1,3-dimethylimidazol- 2-ylidene]silver(I) nitrate and bis[4,5-dichloro-1,3- dimethylimidazol- 2-ylidene]silver(I) nitrate and displayed similar antitumor efficacy against H460 lung cancer cells but less cytotoxic than cisplatin [28]. More recently, a series of Au(I)–NHC complexes of benzimidazol-2-ylidene ware designed by Ott and they showed potency against nontumorigenic cell lines HEK-293 human embryonic kidney cells and HFF human foreskin fibroblasts [7,37]. We developed benzimidazol-2-ylidene based Au(I)–NHC complexes, however, the IC_{50} values of the tested complex [13] were nearly thrice higher than those of cisplatin on B16F10 (mouse melanoma), HepG2 (human hepatocarcinoma) and HeLa (human cervical carcinoma) cell lines. Prominent morphological changes (such as cell rounding and shrinkage and nuclear fragmentation), confirmed cell death is mostly *via* apoptosis. Interestingly, these complexes did not show any significant cytotoxic effects on normal human peripheral blood mono nuclear cells at 100 μM, whereas cisplatin showed 75% cytotoxicity at 10 μM. Our recent work of Au(I)–NHC of pyridine wingtip annelated ligand [11] shows that, complexes are very potent against HepG2 (human hepatocellular carcinoma), HCT 116 (human colorectal carcinoma), A549 (human

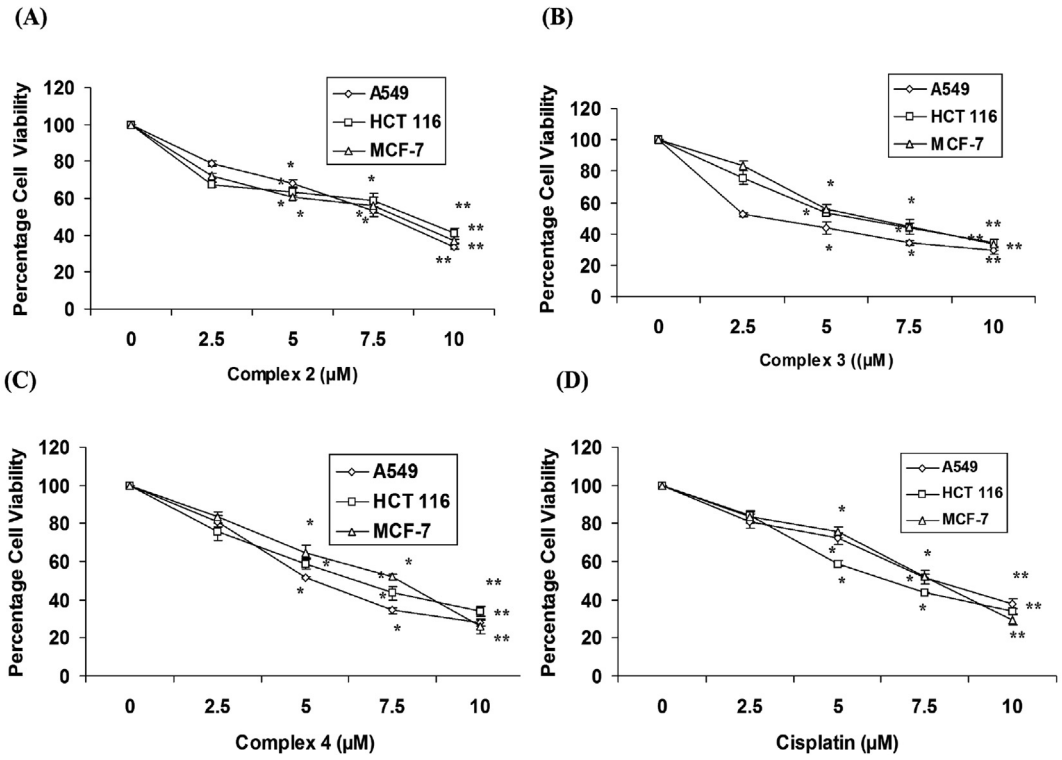

Fig. 4. Cell viability assay: 1×10^4 cells were treated with cisplatin or complexes **2**–**4** (0–10 μM) for 24 h and MTT assay was performed. Values are mean ± S.D. and represent one of the three representative experiments. *P < 0.05 and **P < 0.01.

lung adenocarcinoma), and MCF-7 (human breast adenocarcinoma) having IC_{50} values 3.6 ± 4.1–5.2 ± 1.5 μM. Gautier and other developed a series of Au(I)–NHC complexes which displayed IC_{50} in the same range as cisplatin and continuous studies are underway to find better activities of gold complexes [39–41]. In addition to the Au(I)–NHC complexes, Au(III)–NHC complexes also recently attracted attention due to their strong anticancer activities [11,13,36,38]. As Au(III) and Pt(II) are isoelectronic and they have square planer geometry one expected it would be nice choice of Au(III) as alternative as many cases cisplatin is resistive towards a series cancer cell lines. Guest's group has shown that Au(III)–NHC complexes of 4,5-diarylimidazolidene are very potent against MCF-7, HT-29, HCT-116 and HEP-G2 Cells [42], But it is also observed in many cases Au(III)–NHC are less potent than corresponding Au(I)–NHC complexes as Au(III) finally reduced to Au(I) under physiological condition [13]. Present Au(III) compound, **4** is lees potent than reported Au(III)–NHC by our group; probably bulky naphthyl group prohibit to enter into the cell which is the reason of lower potency. Details mechanism is need for clarification which is further scope of studies.

Table 3
IC_{50} (μM) of cancer cells in presence of cisplatin, ligand **1**, and complexes **2**–**4** after 24 h.

Compound	A549	HCT-116	MCF7	PBMCs
1	>10	>10	>10	>10
2	9.2 ± 2.5	>10	8.78 ± 1.75	>10
3	3.2 ± 0.78	5.2 ± 1.2	6.78 ± 1.82	>10
4	5.2 ± 1.25	6.78 ± 2.01	7.72 ± 2.25	>10
Cisplatin	9.17 ± 2.78	7.2 ± 1.98	8.1 ± 1.32	6.28 ± 2.11

Cells were treated with different concentrations of cisplatin, ligand **1**, and complexes **2**–**4** ranging from 0 to 10 μM for 24 h. IC_{50} (μM) values were calculated from MTT assay. Values are mean ± S.D and represent one of the three representative experiments.

*2.4.2. Apoptosis inducing potential of complex **3***

The apoptosis inducing potential of complex **3** was investigated on A549 cells owing to its high growth inhibitory potential towards it. A549 cells were treated with complex **3** for 24 h and then stained with the nuclear staining dye 4,6-diamidino-2-phenylindole (DAPI). The cells showed rounding of cellular morphology and chromatin condensation along with nuclear fragmentation as compared to the control cells (Fig. 5), all of which are the hallmarks of apoptosis [24].

Phosphatidylserine [PS] externalization from inner cell membrane to outer membrane is the prerequisite for apoptosis.

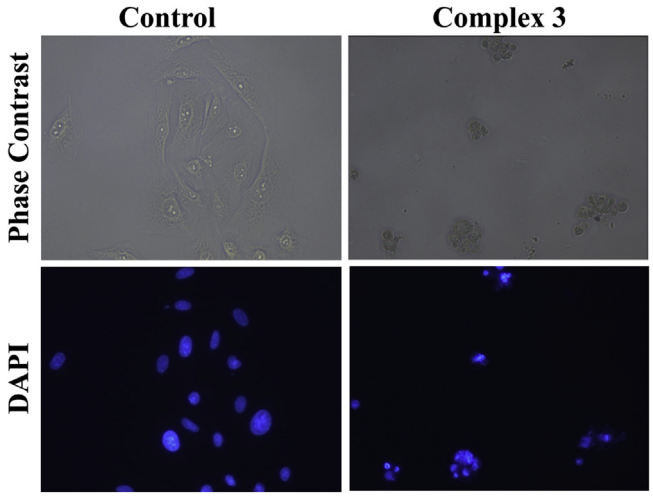

Fig. 5. Fluorescent micrographs of the A549 cells following treatment with complex **3** (IC_{50} concentration) for 24 h and subsequent staining with DAPI. magnification at 20×.

Externalized PS can bind with annexin V. In parallel, the A549 cells were exposed to FITC labeled Annexin V and monitored by flow cytometric analysis. A549 cells treated with complex **3** (IC_{50} concentration) showed apoptotic cell population at 35.94%, significantly higher than the 0.45% s compared to 1.01% measured in the control cells after 24 h (Fig. 6). Collectively, these results were consistent with the occurrence of apoptosis [43] (Chart 1).

3. Conclusion

We have described the synthesis of the annelated proligand precursor 1-naphthyl-2-pyridin-2-yl-2*H*-imidazo[1,5-*a*]pyridin-4-ylium hexafluorophosphate (**1**·HPF_6) and its Ag(I), Au(I) and Au(III)–NHC complexes **2**, **3** and **4**. Solid state structure of Ag(I)–NHC, **2** has been obtained. Cytotoxicities of **2**, **3** and **4** have been studied on non small lung carcinoma (A549), colorectal carcinoma (HCT-116) and breast adenocarcinoma (MCF-7) cell lines. Au (I)–NHC designated Complex **3** showed highest cytotoxicity in A549 cells. Complex **3** induced apoptosis in A549 cells with Phosphatidylserine externalization as highlighted by Annexin-FITC binding and chromatin condensation following DAPI staining. The detailed mechanism of apoptosis would be studied further.

4. Experimental

4.1. General procedures

The following reagents were purchased from Sigma Aldrich, UK and used without additional purification: Ag_2O, NH_4PF_6 and pyridine-2-carboxaldehyde. α-Naphthylamine was purchased from Loba, India. $Au(SMe_2)Cl$ was prepared according to a previously reported procedure [44]. All manipulations were carried out under ambient atmosphere. ^1H NMR and ^{13}C NMR spectra were recorded on a Bruker 300 and 100.5 MHz spectrometers respectively at 25 °C using tetramethylsilane as an internal standard. Cells were obtained from NCCS, Pune. Dulbecco's Modified Eagle Medium (DMEM), fetal bovine serum (FBS), penicillin streptomycin neomycin (PSN) antibiotic, trypsin and ethylenediaminetetraacetic acid (EDTA) were obtained from Gibco BRL (Grand Island, NY, USA). Tissue culture plastic wares were obtained from NUNC (Rokskidle, Denmark). DAPI (4,6-diamidino-2-phenylindole dihydrochloride) was obtained from Invitrogen, California. 3-(4,5-Dimethylthiazol-2-yl)-2,5-diphenyltetrazolium bromide (MTT) was obtained from SRL, India.

4.2. Synthesis of 2-(1-naphthyl)-2H-imidazo[1,5-a]pyridin-4-ylium hexafluorophosphate (1·HPF_6)

The ligand was synthesized following a procedure reported earlier [19]. The corresponding Schiff's base, N-((pyridin-2-yl) methylene)-1-naphthylamine (600 mg, 3.05 mmol), and crushed 91% paraformaldehyde powder (123 g, 4.10 mmol) were taken in 20 mL dioxane and stirred for 6 h to form a slurry. Then the mixture was refluxed for 10 h. After isolation of the aqueous phase, saturated NH_4PF_6 solution was added to get the PF_6 salt which was recrystallised from acetonitrile and diethyl ether. Yield was 746 mg (2.10 mmol, 68.9%). .

^1H NMR (DMSO-d_6, 25 °C, 300 MHz): δ 10.20 (s, 1H, H^a), 8.66 (s, 1H, H^f), 8.34 (d, J = 7.8 Hz, 1H, H^b), 8.22 (d, J = 7.7 Hz, 1H, H^e), 7.95 (m, 2H, $H^{m,\,h}$), 7.77 (m, J = 7.0 Hz, 5H, $H^{c,d,h,k,l}$), 7.41 (d, J = 7.5 Hz, 1H, H^i), 7.34 (d, J = 7.7 Hz, 1H, H^j). ^{13}C NMR (CD_3CN,100.5 MHz): 148.5, 145.7, 140.1, 130.0, 125.5, 125.1, 121.6, 117.6, 116.0, 114.6, 113.4, 112.5, 111.8, 111.4, 111.0, 111.3, 109.2. Anal. Calcd. For $C_{17}H_{13}N_2PF_6$, C, 52.31; H, 3.33; N, 7.18. Found C, 52.09; H, 3.28; N, 7.01%.

4.3. Preparation of 2-(1-naphthyl)imidazo-3-ylidene silver(I) hexafluorophosphate, [Ag(1)$_2$](PF$_6$), **2**

The respective proligand **1.HPF$_6$** (250 mg, 0.64 mmol) and silver oxide (76 mg, 0.33 mmol) were taken in acetonitrile (25 mL) and the mixture was stirred for 4.5 h. After filtering through celite, the volatiles were removed under reduced pressure to get a solid mass. Analytically pure samples were obtained after crystallization from slow diffusion of diethyl ether into acetonitrile solution of complex. Yield was 72% (172.5 mg, 0.23 mmol). ^1H NMR (DMSO-d_6, 25 °C, 300 MHz): δ 8.69 (d, J = 7.8 Hz, 2H, H^b), 8.67 (s, 2H, H^f), 8.24 (d, J = 7.7 Hz, 2H, H^e), 7.97 (m, 4H, $H^{m,\,h}$), 7.78 (m, J = 7.2 Hz, 10H, $H^{c,d,h,k,l}$), 7.44 (d, J = 7.6 Hz, 2H, H^i), 7.35 (d, J = 7.7 Hz, 2H, H^j). ^{13}C NMR (CD_3CN,100.5 MHz): 172.2, 152.4, 148.7, 142.3, 133.1, 127.4, 126.7, 123.5, 119.6, 117.6, 116.6, 114.6, 113.6, 113.8, 112.7, 112.4, 110.3. Anal. Calcd. For $C_{34}H_{24}N_4AgPF_6$, C, 55.07; H, 3.24; N, 7.56. Found C, 54.96; H, 3.25; N, 7.52%.

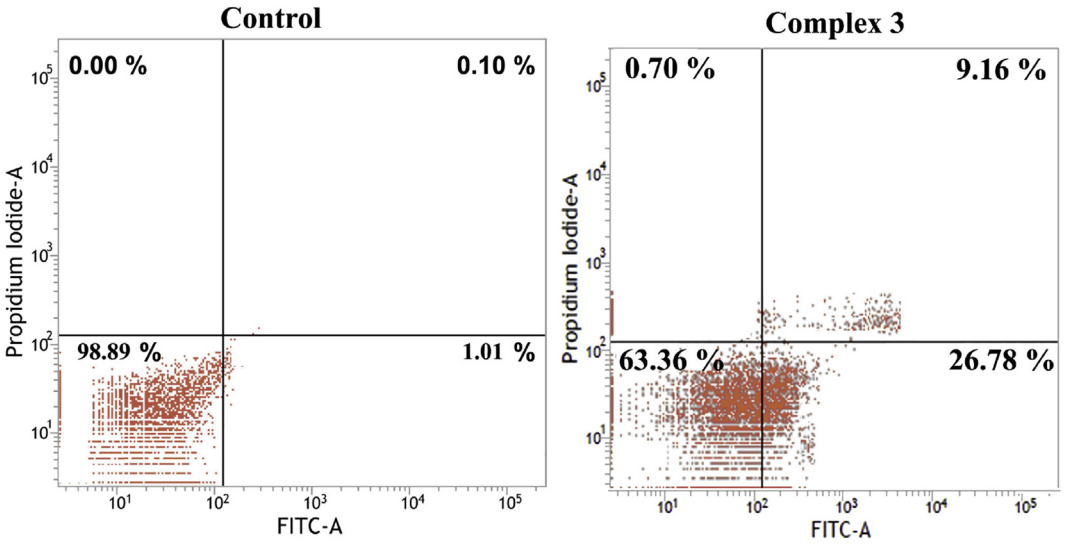

Fig. 6. Flow cytometry analysis of apoptosis induction in A549 cells treated with complex **3** (IC_{50} concentration) for 24 h.

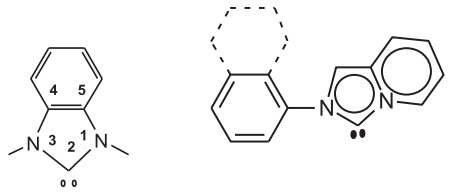

Chart 1. Annelated ligands.

4.4. Preparation of 2-(1-naphthyl)imidazo-3-ylidene gold(I) hexafluorophosphate, [Au(1)$_2$](PF$_6$), **3**

The salt **1·HPF$_6$** (250 mg, 0.64 mmol) and silver oxide (76.4 mg, 0.33 mmol) were dissolved in acetonitrile (25 ml) and the mixture was stirred for 4.5 h. The resulting solution was filtered through a plug of celite to remove the unreacted Ag_2O and the volume of the solvent was reduced to 10 mL. A concentrated acetonitrile solution of Au(SMe_2)Cl (108 mg, 0.37 mmol) was then added dropwise to the silver containing mixture. An immediate white precipitate of AgCl formed and was subsequently removed through filtration; the solvent was then removed. Following drying of the resulting solid, the desired compound was obtained after recrystallization from CH_3CN/Et_2O in 70% yield (188 mg, 0.26 mmol). ^{1}H NMR (DMSO-d$_6$, 25 °C, 300 MHz): δ 8.75 (d, J = 7.8 Hz, 2H, H^b), 8.68 (s, 2H, H^f), 8.25 (d, J = 7.7 Hz, 2H, H^e), 7.99 (m, 4H, H$^{m,\ h}$), 7.81 (m, J = 7.2 Hz, 10H, H^{c,d,h,k,l}), 7.45 (d, J = 7.6 Hz, 2H, H^i), 7.36 (d, J = 7.7 Hz, 2H, H^j). ^{13}C NMR (CD_3CN,100.5 MHz): 174.3, 152.8, 149.4, 142.8, 133.6, 127.7, 126.9, 123.9, 119.8, 117.7, 116.8, 114.7, 113.7, 113.9, 112.8, 112.6, 110.4. Anal. Calcd. For $C_{34}H_{24}N_4$ AuPF$_6$, C, 49.45; H, 2.9?; N, 6.78. Found C, 49.38; H, 2.91; N, 6.70%.

4.5. Preparation of 2-(1-naphthyl)imidazo-3-ylidene gold(III) chloride, [Au(1)Cl$_3$], **4**

To a solution of complex **3** (200 mg, 0.27 mmol) in acetonitrile (10 mL) at room temperature, Au(SMe_2)Cl (160 mg, 0.54 mmol) was added and the resulting mixture was stirred for an additional 5–6 h. The colour of the solution changed from colourless to yellow and this was accompanied by the formation of a small amount of precipitate. The precipitate was presumed to be metallic gold and reused to synthesize Au(SMe_2)Cl. After filtration, the residual acetonitrile was removed under reduced pressure and at low temperature to obtain a yellow powder. The yellow complex was recrystallized from acetonitrile and diethyl ether to obtain the desired compound in 60% yield (89 mg, 0.16 mmol). ^{1}H NMR (DMSO-d$_6$, 25 °C, 300 MHz): δ 8.81 (d, J = 8.1 Hz, 1H, H^b), 8.69 (s, 1H, H^f), 8.26 (d, J = 7.8 Hz, 1H, H^e), 8.01 (m, 2H, H$^{m,\ h}$), 7.82 (m, J = 7.3 Hz, 5H, H^{c,d,h,k,l}), 7.46 (d, J = 7.7 Hz, 1H, H^i), 7.37 (d, J = 7.8 Hz, 1H, H^j). ^{13}C NMR (CD_3CN,100.5 MHz): 175.4, 153.1, 149.6, 143.0, 133.8, 127.8, 127.0, 124.2, 120.1, 117.8, 116.9, 114.9, 113.8, 114.1, 112.9, 112.7, 110.6. Anal. Calcd. For $C_{17}H_{12}N_2$ AuCl$_3$, C, 37.26; H, 2.19; N, 5.11. Found C, 37.12; H, 2.16; N, 5.06%.

4.6. X-ray crystallography

Crystals of **1** and **3** were grown by diffusion of diethyl ether into a solution of the respective compound in acetonitrile. The crystal data and details of the data collections for **1** and **3** are given in Table 1. X-ray data were collected on a CCD diffractometer (graphite monochromated Mo Ka radiation, k = 0.71073 Å) by use of ω scans. The structures were solved by direct methods and refined on F2 using all reflections with SHELX-97 [45]. The nonhydrogen atoms were refined anisotropically. Hydrogen atoms which were not bound to imidazolium-C2 atoms were placed in calculated positions and assigned to an isotropic displacement parameter of 0.08 Å.

4.7. Cell culture

Cell lines, such as HCT-116 (human colorectal carcinoma), MCF-7 (human breast adenocarcinoma), and A549 (human non small lung carcinoma) were obtained from National Centre for Cell Sciences, Pune, India. The cell lines were cultured in DMEM supplemented with 10% FBS and 1% antibiotic (PSN), and incubated at 37 °C in a humidified atmosphere with 5% CO_2. After achieving 75–80% confluence, cells were harvested with 0.025% trypsin and 0.52 mM EDTA (Ethylenediaminetetraacetic acid) in phosphate buffered saline (PBS) and were seeded at desired density to allow them to re-equilibrate a day before the start of experimentation. All experiments were conducted in DMEM supplemented with 10% FBS and 1% antibiotic (PSN) solution.

4.8. In vitro cytotoxicity assay

Cells were cultured according to the American Type Culture Collection (ATCC) manufacturer's instructions. Cells were maintained at 37 °C and 5% CO_2 in a humidified incubator. The 3-(4,5-Dimethylthiazol-2-yl)-2,5-diphenyltetrazolium bromide (MTT) assay has used for the measurement of cytotoxicity of these complexes. Cells (3000/well) were plated in 96-well culture plates 24 h prior to the complex treatment. The cell lines were treated with the (0, 2.5, 5 and 10 μM) of complexes **2**, **3** and **4** for 24 h. In parallel, the cells were treated with 0.5% (v/v) DMSO and considered as a control, since the complexes were dissolved in DMSO. At the end of incubation, MTT (20 μl of 5 mM MTT solution) was added in each well and further incubated for 4 h in cell culture incubator. Then the medium was replaced with 150 μl of MTT solvent (4 mM HCl, 0.1% NP-40 in isopropanol) and further incubated for 15 min at room temperature. Finally, the absorbance readings at 595 nm were collected in Elisa plate reader (Bio-Rad, Model 680XR) as described earlier (24). The data from cancer cell lines were acquired from three independent cell passages. The IC$_{50}$ values were calculated from the plot of cell viability *vs* concentration of complexes.

4.9. Assessment of cellular death parameters under a microscope

A549 cells treated with complex **3** (IC$_{50}$ concentration) for 24 h were viewed under a phase contrast microscope. Cells were stained with DAPI (4′, 6-diamidino-2-phenylindole) for the detection of chromatin condensation and DNA fragmentations, and were observed under an inverted phase contrast/fluorescent microscope (Model: OLYMPUS IX70, Olympus Optical Co. Ltd., Shibuya-ku, Tokyo, Japan); images were acquired as described earlier [24].

4.10. Detection of apoptosis using flow cytometry

Apoptosis was assayed by using an annexin V-FITC apoptosis detection kit (Calbiochem, La Jolla, CA) as described earlier [24]. A549 cells treated with complex **3** (IC$_{50}$ concentration) for 24 h were stained with PI and annexin V-FITC according to manufacturer's instructions. The percentages of live, apoptotic and necrotic cells were analyzed by BD LSRFortessa cell analyzer (Becton Dickinson, San Jose, CA, USA). Data from 10,000 events were analyzed for each sample as described earlier [24].

Acknowledgments

JD thanks to Prof. A.A. Danopoulos and Managing Director ITM University Gwalior for constant encouragement. S. A. extends sincere appreciation to the deanship of scientific research at King Saud University for its funding through Prolific Research group (PRG-1436 - 03).

References

[1] A.J. Arduengo III, R.L. Harlow, M.A. Kline, J. Am. Chem. Soc. 113 (1991) 361–363.
[2] D. Bourissou, O. Guerret, F.P. Gabbai, G. Bertrand, Chem. Rev. 100 (2000) 39–91.
[3] P. De Fremont, N. Marion, S.P. Nolan, Coord. Chem. Rev. 253 (2009) 862–892.
[4] B.M. Neilson, C.W. Bielawski, J. Am. Chem. Soc. 134 (2012) 12693–12699 and references therein.
[5] A.S.K. Hashmi, A.M. Schuster, F. Rominger, Angew. Chem. Int. Ed. 48 (2009) 8247–8249.
[6] W. Liu, R. Gust, Chem. Soc. Rev. 42 (2013) 755–773.
[7] L. Oehninger, R. Rubbiani, I. Ott, Dalton Trans. 42 (2013) 3269–3284.
[8] B. Rosenberg, L. Vancamp, J.E. Trosko, V.H. Mansour, Nature 222 (1969) 385–386.
[9] A. Kascatan-Nebioglu, M.J. Panzner, C.A. Tessier, C.L. Cannon, W.J. Youngs, Coord. Chem. Rev. 251 (2007) 884–895.
[10] N.H. Kim, H.J. Park, M.K. Oh, I.S. Kim, BMB Rep. 46 (2013) 59–64.
[11] B.K. Rana, A. Nandy, V. Bertolasi, C.W. Bielawski, K.D. Saha, J. Dinda, Organometallics 33 (2014) 2544–2548.
[12] C.F. Shaw III, Chem. Rev. 99 (1999) 2589–2600.
[13] S.D. Adhikary, D. Bose, P. Mitra, K.D. Saha, V. Bertolasi, J. Dinda, New. J. Chem. 36 (2012) 759–767.
[14] H.M.J. Wang, I.J.B. Lin, Organometallics 17 (1998) 972–975.
[15] J. Dinda, S.D. Adhikary, S.K. Seth, A. Mahapatra, New. J. Chem. 37 (2013) 431–438.
[16] L. Benhamou, E. Chardon, G. Lavigne, S.B. Laponnaz, V. Cesar, Chem. Rev. 111 (2011) 2705–2733.
[17] W.A. Hermann, Angew. Chem. Int. Ed. 41 (2002) 1290–1309.
[18] T. Samanta, S.K. Seth, S.K. Chattopadhyay, P. Mitra, V. Kushwah, J. Dinda, Inorg. Chim. Acta 411 (2014) 165–171.
[19] T. Samanta, B.K. Rana, G. Roymahapatra, S. Giri, P. Mitra, R. Pallepogu, P.K. Chattaraj, J. Dinda, Inorg. Chim. Acta 375 (2011) 271–279.
[20] D. Das, J. Dinda, T. Mondal, C. Sinha, J. Indian Chem. Soc. 83 (2006) 603–607.
[21] J. Dinda, T. Samanta, A. Nandy, K. Das Saha, S.K. Seth, S.K. Chattopadhyay, C.W. Bielawski, New. J. Chem. 38 (2014) 1218–1224.
[22] R. Visbal, A. Laguna, M.C. Gimeno, Chem. Commun. 49 (2013) 5642–5644.
[23] GAUSSIAN 03, Revision B.03; GAUSSIAN Inc., Pittsburgh, PA.
[24] A. Nandy, S.K. Dey, S. Das, R.N. Munda, J. Dinda, K.D. Saha, Mol. Cancer. 13 (2014) 1–14.
[25] J.C.Y. Lin, R.T.W. Huang, C.S. Lee, A. Bhattacharyya, W.S. Hwang, I.J.B. Lin, Chem. Rev. 109 (2009) 3561–3598.
[26] G. Roymahapatra, S.M. Mandal, W.F. Porto, T. Samanta, S. Giri, J. Dinda, O.L. Franco, P.K. Chattaraj, Curr. Med. Chem. 19 (2012) 4184–4193.
[27] J.C. Garrison, W.J. Youngs, Chem. Rev. 105 (2005) 3978–4008.
[28] K.M. Hindi, T.J. Siciliano, S. Durmus, M.J. Panzner, D.A. Medvetz, D.V. Reddy, L.A. Hogue, C.E. Hovis, J.K. Hilliard, R. Mallett, C.A. Tessier, C.L. Cannon, W.J. Youngs, J. Med. Chem. 51 (2008) 1577–1583.
[29] N.H. Kim, H.J. Park, M.K. Oh, I.S. Kim, BMB Rep. 46 (2013) 59–64.
[30] C.F. Shaw III, Chem. Rev. 99 (1999) 2589–2600.
[31] N. Marion, S.T. Díez-Gonźalez, S.P. Nolan, Angew. Chem. Int. Ed. 119 (2007) 3046–3058.
[32] P.J. Barnard, S.J. Berners-Price, Coord. Chem. Rev. 2519 (2007) 1889–1902.
[33] S. Ray, R. Mohan, J.K. Singh, M.K. Samantaray, M.M. Shaikh, D. Panda, P. Ghosh, J. Am. Chem. Soc. 129 (2007) 15042–15053.
[34] J.L. Hickey, R.A. Ruhayel, P.J. Barnerd, M.V. Baker, S.J. Berners-Price, A. Filipovska, J. Am. Chem. Soc. 30 (2008) 12570–12571.
[35] E. Schuh, C. Pflüger, A. Citta, A. Folda, M.P. Rigobello, A. Bindoli, A. Casini, F. Mohr, J. Med. Chem. 55 (2012) 5518–5528.
[36] T. Zou, C.T. Lum, S.S.-Y. Chui, C.-M. Che, Angew. Chem. Int. Ed. 52 (2013) 2930–2933.
[37] R. Rubbiani, S. Can, I. Kitanovic, H. Alborzinia, M. Stefanopoulou, M. Kokoschka, S. Mönchgesang, W.S. Sheldrick, S. Wölfl, I. Ott, J. Med. Chem. 54 (2011) 8646–8657.
[38] J. Dinda, A. Nandy, B.K. Rana, V. Bertolasi, K.D. Saha, C.W. Bielawskie, RSC Adv. 4 (2014) 60776–60784.
[39] A. Gautier, F. Cisnetti, Metallomics 4 (2012) 23–32.
[40] M.-L. Teyssot, A.-S. Jarrousse, M. Manin, A. Chevry, S. Roche, F. Norre, C. Beaudoin, L. Morel, D. Boyer, R. Mahiou, A. Gautier, Dalton Trans. 35 (2009) 6894–6902.
[41] [a] B. Bertrand, A. Casini, Dalton Trans. 43 (2014) 4209–4219 and ref. therein; [b] M.E. Garner, W. Niu, X. Chen, I. Ghiviriga, K.A. Abboud, W. Tan, A.S. Veige, Dalton Trans. 44 (2015) 1914–1923; [c] Y. Li, G.-F. Liu, C.-P. Tan, L.-N. Ji, Z.–W. Mao, Metallomics 6 (2014) 1460–1468.
[42] W. Liu, K. Bensdorf, M. Proetto, U. Abram, A. Hagenbach, R. Gust, J. Med. Chem. 54 (2011) 8605–8615.
[43] S. Mallick, B.C. Pal, J.R. Vedasiromoni, D. Kumar, K.D. Saha, Cell. Physiol. Biochem. 30 (2012) 915–926.
[44] R. Uson, A. Laguna, M. Laguna, Inorg. Synth. 26 (1989) 85–91.
[45] G.M. Sheldrick, SHELX-97, Program for Crystal Structure Refinement, University of Gottingen, Germany, 1997.